Applied Chemical Engineering (2023) Volume 6 Issue 3
doi: 10.24294/ace.v6i3.2009

ORIGINAL RESEARCH ARTICLE

Morphology based catalytic oxidation of phenylpropyne into 1,2-diketones, aldehyde and acid using Cu(II) complex

Prashant Kaushik[1], Nidhi Malik[2], Prashant Tevatia[1], Vinod Kumar[3], Prasanta Kumar Sahu[4], Ravinder Kumar[1,*]

[1] *Department of Chemistry, Gurukula Kangri (Deemed to be University), Haridwar 249404, India*

[2] *School of Engineering and technology, The Northcap University, Gurugram 122017, India*

[3] *Special Centre for Nano Sciences, Jawaharlal Nehru University, Delhi 110067, India*

[4] *Department of Chemistry, Shivaji College, University of Delhi, Delhi 110007, India*

*** Corresponding author:** Ravinder Kumar, ravinder.kumar@gkv.ac.in

ABSTRACT

Aldehyde, 1,2-diketones, and acid were prepared by copper-catalyzed oxidation of phenyl propyne, using t-BuOOH as the oxidant, heterogeneously. Aldehyde is formed as a major product under neutral conditions. Under mild conditions, catalysis was carried out using catalytic amounts of [Cu(L)Br] with N-methyl benzimidazolyl Schiff base ligand and stoichiometric amounts of oxidant in CH_3CN. The several properties of the catalyst were characterized by using UV-Vis, FT-IR, PXRD, CV, and Electron paramagnetic resonance techniques. Comparative SEM measurement of catalyst before and after the catalysis shows that the morphology and size of rods affect the catalytic efficiency. The percentage yields of products were determined by GC-MS.

Keywords: Copper complex; *N*-methyl benzimidazolyl Schiff base; phenylproyne; heterogeneous catalysis

ARTICLE INFO

Received: 31 March 2023
Accepted: 14 September 2023
Available online: 17 November 2023

1. Introduction

Now a days diketones, aldehyde, alcohol, and acid have various application in pharmaceutical chemistry, flavouring industry, cosmetics industry, fragrances and flavors, organic transformation etc.[1–10]. Due to wide application in diverse field it is important to prepare. Previous studies suggest the formation of 1,2-diketone from the oxidation of alkynes is the most common and useful phenomenon[11–16]. The 1,2-diketones have numerous biological activities[15,16] due to their structural moieties[17,18] and they also act as precursors for various ligands like diols[19], NHC[20] and diamines[21]. These compounds are largely used for the production of expanded compounds[22] and also utilized as photoinitiators in the curing of polymer networks[23]. Wacker process, epoxidation and allylic oxidation results in the formation of aldehyde, ketone, and corresponding acid that are important precursors and used for the preparation of valuable intermediates that are extensively used in agriculture, medicine, and fine chemical industry[24–28]. Various copper(II) complex is used for selective oxidation of olefins homogeneous[29–31] and heterogeneously[32–34] using TBHP and H_2O_2 as oxidants. The copper based catalyst for the oxidation of alkynes has not been much explored to date[35–39]. Oxidation of alkynes using the Cu-catalyzed mechanism is highly efficient[40]. In recent years, researchers focus to develop simple, effective, and eco-friendly

catalysts[41] for the oxidation process along with growing interest in promoting heterogeneous catalysts[42]. Here, we describe a method to synthesize diketones, aldehyde and acid from phenylpropyne using t-BuOOH as an oxidant, and using Cu(II) complex of *N*-methyl benzimidazolyl Schiff base ligands, heterogeneously. So we design a catalyst that is used to prepare aldehyde, ketones and acid in a selective manner, heterogeneously. We also focus on changing the catalytic properties during catalysis by using SEM. We also analyzed the morphology and identification of the lattice of reused catalyst using SEM and PXRD techniques

2. Experimental section

2.1. Materials and method

Glycine-98%(Merck), N-Methyl-o-Phenylenediamine-98% (Thomas Baker), K_2CO_3-99% (Thomas Baker), 1-phenylpropyne-99% (Merck), 2-Hydroxy-1-Naphaldehyde-98% (Alfa-Aesar), $CuBr_2$-99% (Sigma Aldrich) and 70% (t-BuOOH) (Lancaster). (N-Me-GB.2HCl) was prepared[43].

2.2. Synthesis of ligand

The Schiff base ligand [$C_{20}H_{17}N_3O$] was synthesized and single crystal structure of this ligand was obtained in MeCN: MeOH (3:2) as reported earlier is having a CCDC no. 932006[43]. After neutralizing the solution of *N*-methyl 2-aminomethyl benzimidazolyl dihydrochloride by K_2CO_3, solution in methanol of 2-hydroxy-1-naphthaldehyde is slowly added with constant stirring at RT. Yellow solid is separated out after 15 mins of constant stirring. This solid was filtered, dried over P_2O_5 and recrystallized from CH_3CN **Scheme 1**.

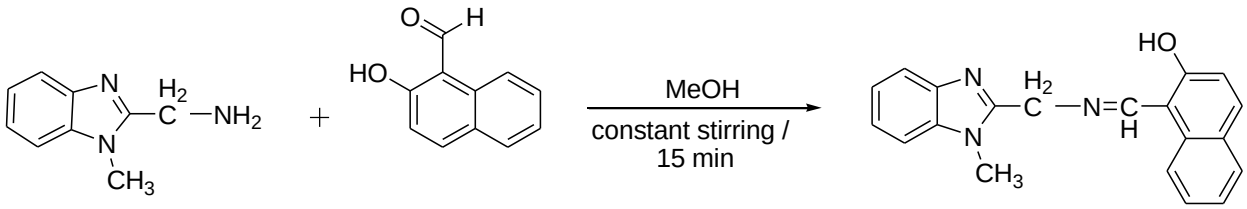

Scheme 1. Synthesis of Schiff base ligand.

2.3. Synthesis of copper complex [Cu(L)Br]

The Ligand (0.317 mmol) are soluble in methanol (10 mL), then add $CuBr_2$ (0.317 mmol), dissolved in minimum amount of methanol at RT. During addition with constant stirring, a green solid product is formed immediately. The product was filtered and air dried in vacuo over P_2O_5. The compound analyzed initially by weighing and taking the melting point $C_{20}H_{16}BrCuN_3O$. Yield: 84%; m.p.: 192 °C.

UV-Vis λ_{max}/nm(log ε) in DMF: 273(4.3), 280(4.3), 317(4.1), 395(3.9), 640(2.1).

Anal. Found (Calc.) for $C_{20}H_{16}N_3OCuBr$: C 51.2(52.4), H 3.3(3.4), N 9.0(9.1).

Selected IR (KBr, cm^{-1}) $\nu_{(-C=N-C=C-)}$ 1419, $\nu_{(NH)(H\text{-bonded})}$ 3164, $\nu_{(C=N)}$ 1619, $\nu_{benzene\ strech}$ 742.

2.4. Instrumentations

IR spectra were recorded in the range of 400–4000cm^{-1}on a Perkin-Elmer FT-IR-2000 spectrometer using KBr discs. Elemental analysis obtained on VARIO EL III from University science instrumentation center, University of Delhi, India. UV-Vis spectra recorded in a Shimadzu UV-Vis-1601 spectrometer in DMF. The morphological changes of the complex were studied using SEM with gold coating (Model FEI Quanta 200F with oxford–EDS system IE 250 X Max 80) in SMITA research lab IIT Delhi, India. GC-MS spectra recorded at AIRF, JNU, New Delhi (GCMS-QP2010 (plus) Schimadzu). The PXRD patterns were recorded over the range of 2θ = 5°–35° using High resolution D8 Discover Bruker diffractometer, equipped

with point detector (scintillation counter), employing monochromatized Cu $K_{\alpha 1}$ radiation with a scan rate of 1.0 second/step and step size 0.02° at 298 K.

3. Results and discussion

3.1. Le-Bail fitting pattern of copper complex

Powder XRD for the Cu(II) complex studied are used for the identification of phase, crystallinity and unit cell dimensions. To determine the nature of bonding or geometry we can do the Le-Bail fitting of observed Powder-XRD pattern of this copper(II) complex are observed by using the crystal parameters of comparable copper(II) complex with CCDC no. is 932004 [Unpublished work[44].

The Le-Bail fitting pattern suggests a ***Triclinic P-1*** symmetry in which the Schiff base ligand is coordinated in a tridentate manner (N,N,O) via the imine N, azomethine (–C=NH–) and a deprotonated oxygen of 2-napthanol. The fourth coordination is occupied by exogenous anion (Br^-) ion, forming distorted square plane. The bond length of copper with exogenous anion (Br^-) is elongated than the remaining three bonds with NNO contributing to the distortion in the square planer geometry[45,46]. **Table 1** shows the value of lattice constants obtained after the Le-Bail fitting. Figure 1 shows the Le-Bail Fitting of the [Cu(L)Br] catalyst.

Table 1. Le-Bail Fitting parameter of the [**Cu(L)Br]** complex.

Crystal	Space group	A	B	c	α	β	Γ
Triclinic	P-1	9.1807	8.2059	10.1717	74.8574	75.2713	64.5944

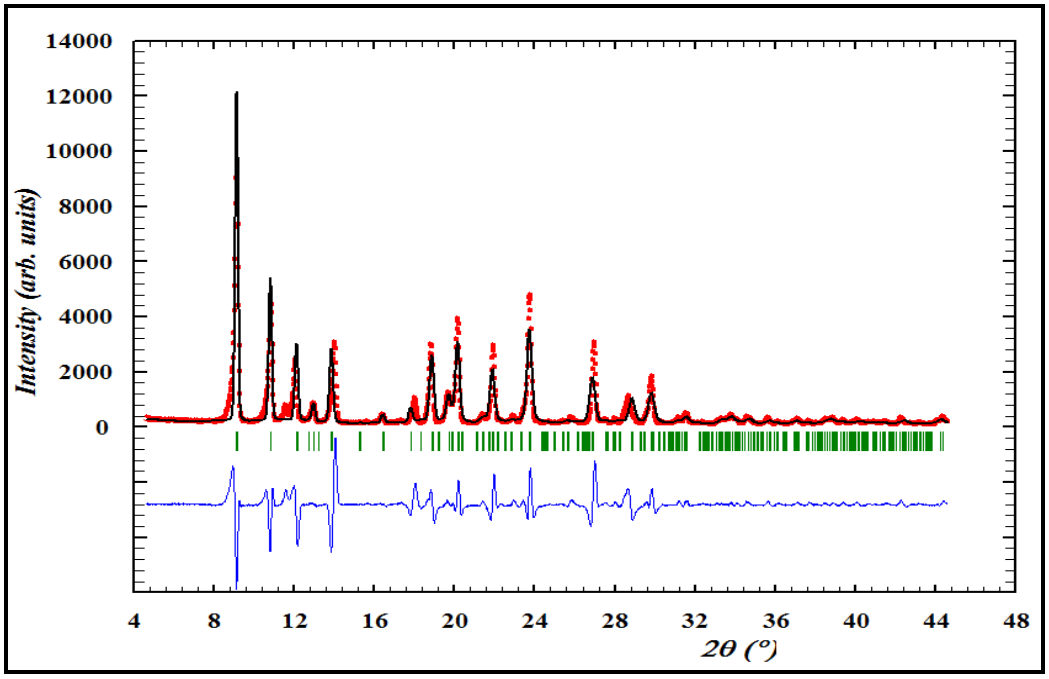

Figure 1. Le-Bail Fitting of the [**Cu(L)Br]** catalyst.

3.2. Electronic spectroscopy and IR studies

The electronic spectral data of the copper complex is given in experimental section. The UV spectra of the ligand show three absorption band in the range of 271–306 nm[43] In complex the band at 273 nm and 280 nm correspond to **π-π*** transition characterizing the benzimidazole group while the band at 317 nm is assign to the **n-π*** transition fuses with an additional broad band due to the LMCT from the napthanol oxygen to a vacant d-orbital of copper ion[47]. Due to d^9 configuration of copper(II) a broad but a much less intense d-d band is observed at 640 nm[43] (**Figure 2**).

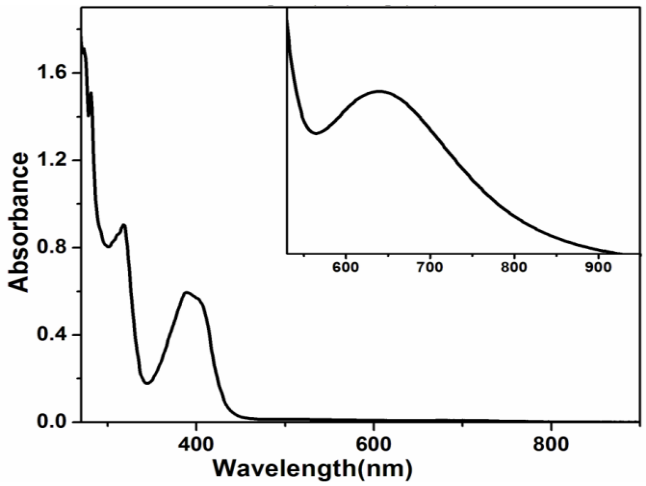

Figure 2. UV-Visible spectra of [Cu(L)Br] catalyst.

The IR spectra of the copper complex has characteristic IR band at 1619 cm^{-1} due to ν (C=N) indicating a coordination of azomethine nitrogen and imine nitrogen to the copper[48–53]. The band between 1419 cm^{-1} and 742 cm^{-1} is assigned to $\nu_{(C=N-C=N)}$ stretching of the benzimidazole group[54]. During complexation, the band moves towards the lower wave number by 20–30 cm^{-1}. The characteristic stretching frequency for the coordination anion is also observed.

3.3. Cyclic voltametric studies

Cyclic voltammograms of the [Cu(L)Br] were studies in a mixture of MeCN: DMSO (3:2) solution with tetrabutylammonium perchlorate (TBAP) as supporting electrolyte at room temperature. The three electrode assembly: (i) glassy carbon as working electrode; (ii) Pt wire as auxiliary electrode; (iii) $Ag/AgNO_3$ as reference electrode. The [Cu(L)Br] shows a quasi-reversible peak for the couple: Cu(II) ↔ Cu(I)[41] (**Figure 3**).

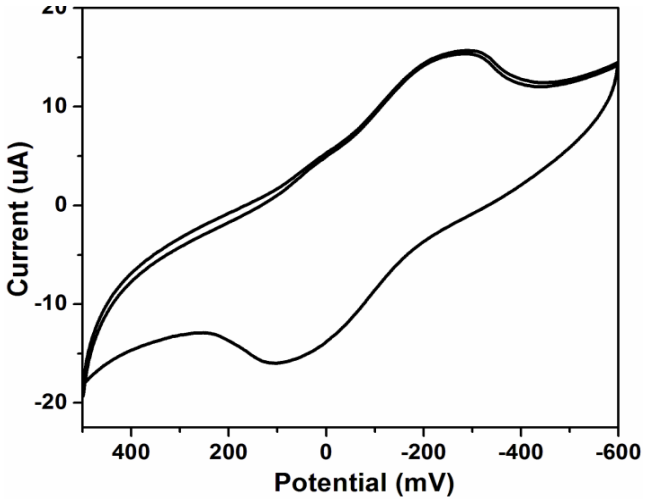

Figure 3. Cyclic Voltammogram Spectra of [Cu(L)Br] catalyst.

3.4. EPR studies

X-Band EPR spectrum of the catalyst was recorded in DMF at 77 K as shown in **Figure 4**. The spin Hamiltonian parameter for the copper complex is calculated from the spectra. The copper nucleus with nuclear spin I = 3/2 for the unpaired electron and produces a hyperfine splitting (2nI+1) into four components. However the present complex, spectra show less than four lines and a broadening of $g_{\perp}$ line, indicating a distortion of the planer geometry[43]. They do not show a four line hyperfine pattern and their EPR spectra have been analyzed as given by Kneubühl[55]. The corresponding g_1 = 2.05 and g_2 = 2.17 values shows that the complex is axial

electronic structure[56]. $g_{\perp} > g_{\parallel}$ indicates an electron lies in $d_{x^2-y^2}$ orbital. g > 2 axial structure its means the anion is attached to Cu^{2+} in axial site[56]. The peak at 3000 G belong to originates from delocalized electrons in the 1Se state[57].

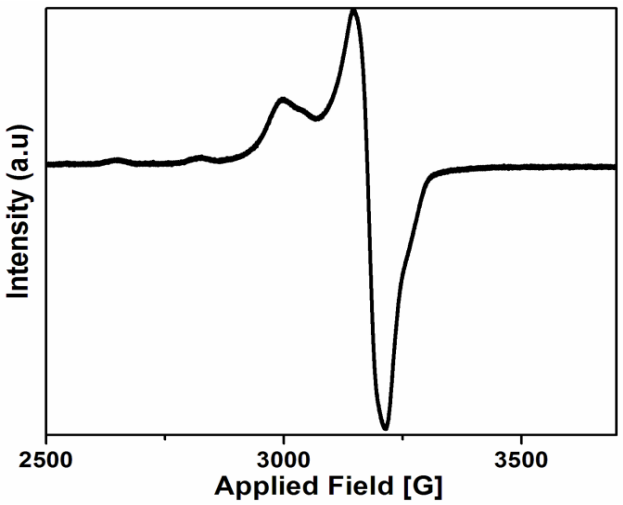

Figure 4. EPR Spectra of [Cu(L)Br] catalyst.

3.5. Catalytic activity studies

The Cu(II) catalyst was used heterogeneously for the oxidation of phenyl propyne to its corresponding carbonyl compound, aldehyde and acid with t-BuOOH as an alternative source of oxygen. In a typical reaction, catalyst (0.0218 mmol), phenyl propyne (0.1092 mmol) and oxidant (0.1092 mmol, 70%) in ratio of [1:5:5] were mixed in 15 mL CH_3CN and stirred at 35 °C–40 °C for 10 hrs. The growth of the reaction was monitored by using TLC. The development of DNP derivative in TLC confirms the formation of corresponding carbonyl compound during reaction. After completion, reaction mixture was centrifuged to isolate the copper(II) catalyst. To checked the dissolution of copper catalyst during catalysis, UV-Vis spectra of the filtrate was taken, no band in the visible range of 500–900 nm was observed ruling out the possibility of any dissolution of the copper(II) catalyst[43]. The clear filtrate was diluted and subjected to GC-MS to analyze the products obtained using naphthalene as an internal standard. To study the effect of pH, we have doen this catalysis in acidic and basic condition by using Acidic buffer (sodium acetate + acetic acid) and basic buffer (ammonia and ammonium chloride). The results shows that the maximum percentage conversion was obtained at pH = 10 that is 69% (**Table 2**). Blank experiments were similarly processed out in absence of catalyst that's shows only 3% conversion while in presence of $CuBr_2$ salt 11% conversion of product take place keeping other similar conditions of reaction is same. Oxidation of alkynes leads to Cu(II)/Cu(I) as the reduction mechanism. The coordination of Cu(II) with C–C triple bond leads the C–H activation and removal of hydrogen and formation of Cu-carbon bond, subsequently electron transmission breaks the Cu-carbon bonds and oxidation take place. In basic medium C–H activation and deprotonation will occurs at faster rate as compared in acidic and neutral condition, so the percentage conversion is greater in basic condition[34] **Scheme 2**.

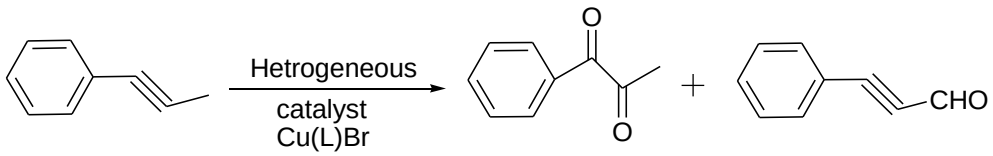

Scheme 2. Oxidation of phenyl propyne to a corresponding diketonic and acetylenic aldehyde.

Table 2. Percentage conversion of products using complex **[Cu(L)Br]** at different condition with (t-BuOOH) as oxidant.

pH	Products	% Conversion	Total conversion (%)
10.0	Ph–CΞC–CHO	37	69%
	Ph–COOH	17	
	Ph–CO–CO–CH_3	15	
7.0	Ph–CΞC–CHO	23	47%
	Ph–COOH	13	
	Ph–CO–CO–CH_3	11	
5.5	Ph–CΞC–CHO	25	52%
	Ph–COOH	15	
	Ph–CO–CO–CH_3	12	

The overall percentage conversion to oxidized products produced by employing tu-BOOH in neutral conditions is 47%, whereas Cu(I)NCS complex of 1-(((1-methyl-1H-benzo[d]imidazol-2-yl)methylimino)methyl)naphthalen-2-ol Schiff base offers 33% conversion in identical conditions. Under basic conditions, the total percentage conversion to oxidized products obtained by using tu-BOOH is 69%, while Cu(II)NO_3 complex of 1-(((1-methyl-1H-benzo[d]imidazol-2-yl)methylimino)methyl)naphthalen-2-ol Schiff base provides 81% conversion under similar conditions. Under acidic conditions, the total percentage conversion from Cu(L)Br is 52%, while Cu(II)NO_3 complex of 1-(((1-methyl-1H-benzo[d]imidazol-2-yl)methylimino)methyl)naphthalen-2-ol Schiff base provides 69% conversion under similar conditions[37].

3.6. SEM Analysis

The effect of morphology on catalytic oxidation of phenylpropyne analyzed using SEM measurement. Initially, the catalyst was found to hold rod-type morphology and the greatest catalytic performance with 69% conversion of phenylpropyne to corresponding diketones, aldehyde and acid was obtained at pH = 10. Most of the rods are flat and the length of rods lies in the ranges of 1.01–1.30 μm (**Figure 5A**). Moreover, to analyze morphological changes of catalyst during catalysis, sample has been prepared through gold coated and analyzed using SEM measurement. After used in the catalytic cycle, 70% of the rods are found to conjoin together, possibly due to augmentation to cluster formation (**Figure 5B**). Subsequently, the reuse of catalyst in catalysis shows 47% conversion under the same condition only. SEM studies showed agglomeration upon reused catalyst decreases the catalytic activity due to changes in the catalyst's surface and it affects the catalytic activity. Therefore, it corroborates that the morphology and exposed crystal face of the catalyst play an important role in an alkynes oxidation reaction and the rod shows superior catalytic activity[58–61].

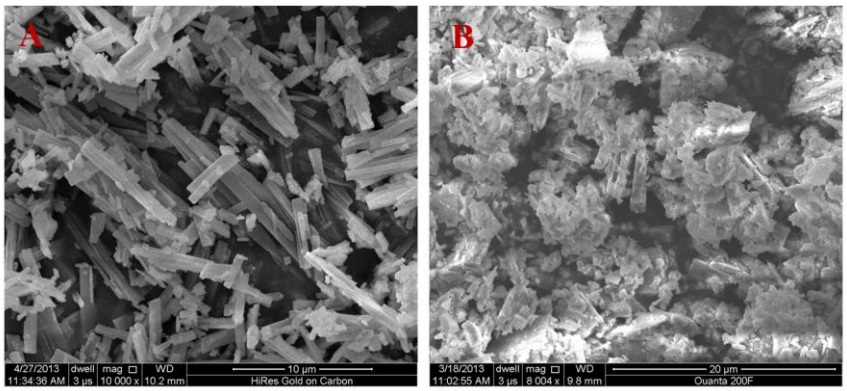

Figure 5. Variation in the morphology of the Cu(L)Br catalyst during catalysis: **(A)** pure catalyst; **(B)** after reaction with phenylpropyne.

4. Conclusion

In summary, we have established a protocol for the production of diketones, aldehydes, and acid from alkynes using copper complex with N-Methyl substituted benzimidazolyl Schiff base ligand having NNO binding sites, heterogeneously. Under mild conditions, relatively safe oxidant, one-pot synthesis, and wide substrate scope render this method a leading substitute to previous approaches. We can reuse this heterogeneous catalyst for the oxidation of alkynes. We found this heterogeneous catalyst efficiently oxidizes internal carbon-carbon triple bonds through the formation of an "oxirene" which undergoes rearrangement and forms diketones and C–H bond activation leads to the creation of aldehyde and corresponding acid. Our result suggests that the synthesized catalyst reacts more rapidly with aromatic alkynes rather than the aliphatic. The percentage conversion shows that the catalytic activity depends upon the morphology of the catalyst and chemical changes. Therefore, it confirms that the importance of the catalyst's morphology and size of rods for the oxidation of aromatic alkynes in the heterogeneous catalysis process.

Author contributions

Conceptualization, RK and VK; methodology, RK and PK; software, RK; NM and PT; validation, VK, and RK, investigation, NM and PKS; resource, PK and VK; writing—original draft preparation, RK, VK and PK; writing—review and editing, RK, NM, PK and VK; visualization, NM, PKS and VK; supervision, RK and VK. All authors have read and agreed to the published version of the manuscript.

Acknowledgments

The authors gratefully acknowledge the department of chemistry and USIC, University of Delhi, Delhi, India for research and instrumentation facility. The authors are highly thankful to Prof. Pavan Mathur, Retired Professor, Department of Chemistry, University of Delhi, Delhi, for his research guidance and valuable suggestions. The author RK is thankful to UGC-BSR project no. 30-496/2019 for financial supports.

Conflict of interest

The authors declare no conflict of interest.

References

1. Verma DK, Al-Sahlany ST, Niamah AK, et al. Recent trends in microbial flavour Compounds: A review on Chemistry, synthesis mechanism and their application in food. *Saudi Journal of Biological Sciences* 2022; 29(3): 1565–1576. doi: 10.1016/j.sjbs.2021.11.010
2. KR R, Gopi S, Balakrishnan P. Introduction to flavor and fragrance in food processing. In: *Flavors and Fragrances in Food Processing: Preparation and Characterization Methods*. American Chemical Society; 2022. pp. 1–19.
3. Maurya R, Patel H, Bhatt D, et al. Microbial production of natural flavors and fragrances. In: *Recent Advances in Food Biotechnology.* Springer, Singapore; 2022. pp. 139–159.
4. Shen D, Wang H, Zheng Y, et al. Catalyst-free and transition-metal-free approach to 1, 2-diketones via aerobic alkyne oxidation. *The Journal of Organic Chemistry* 2021; 86(7): 5354–5361. doi: 10.1021/acs.joc.0c03010
5. Kaushik P, Rawat BS, Kumar R. Various approaches for the synthesis of benzimidazole derivatives and their catalytic application for organic transformation. *Applied Chemical Engineering* 2023; 6(2): 2003. doi: 10.24294/ace.v6i2.2003
6. Bakshi R, Kumar R, Mathur P. Bis-benzimidazole diamide iron (III) complexes as mimics of phenoxazinone synthase. *Catalysis Communications* 2012; 17: 140–145. doi: 10.1016/j.catcom.2011.10.017
7. Kumar R, Mathur P. Aerobic oxidation of 1, 10-phenanthroline to phen-dione catalyzed by copper (II) complexes of a benzimidazolyl Schiff base. *RSC Advances* 2014; 4(63): 33190. doi: 10.1039/c4ra03651d
8. Mahiya K, Kumar R, Lloret F, Mathur P. Oxidation of substituted phenols using copper (II) metallatriangles formed through ligand sharing. *Spectrochimica Acta Part A: Molecular and Biomolecular Spectroscopy* 2014; 133: 663–668. doi: 10.1016/j.saa.2014.06.026

9. Ni Z, Padilla R, dos Santos Mello L, Nielsen M. Tuning Ethanol Upgrading toward Primary or Secondary Alcohols by Homogeneous Catalysis. ACS Catal. 2023; 13(8): 5449–55. doi: https://doi.org/10.1021/acscatal.2c06322
10. Tyagi N, Kumar R, Mahiya K, Mathur P. Copper (II) complexes of a new tetradentate bis-benzimidazolyl diamide ligand with disulfanediyl linker: synthesis, characterization, and oxidation of some pyridyl, napthyl, and benzyl alcohols. *Journal of Coordination Chemistry* 2013; 66(19): 3335–3348. doi: 10.1080/00958972.2013.835403
11. Liu YP, Guo JM, Yan G, et al. Anti-inflammatory and antiproliferative prenylated isoflavone derivatives from the fruits of *Ficus carica*. *Journal of Agricultural and Food Chemistry* 2019; 67(17): 4817–4823. doi: 10.1021/acs.jafc.9b00865
12. Zhang J, Zhang C, Xu FC, et al. Cholinesterase inhibitory isoquinoline alkaloids from Corydalis mucronifera. *Phytochemistry* 2019; 159: 199–207. doi: 10.1016/j.phytochem.2018.11.019
13. Wu C, Liang Z, Yan D, He W, Xiang. Straightforward and highly efficient synthesis of α-acetoxy ketones through gold-catalyzed intermolecular oxidation of terminal alkynes. *Synthesis* 2013; 45(18): 2605–2611. doi: 10.1055/s-0033-1338513
14. Jiang HF, Tang JY, Wang AZ, et al. Cu (II)-promoted oxidative homocoupling reaction of terminal alkynes in supercritical carbon dioxide. *Synthesis* 2006; (7): 1155–1161. doi: 10.1055/s-2006-926372
15. Worayuthakarn R, Boonya-Udtayan S, Ruchirawat S, Thasana N. Total synthesis of unsymmetrical benzils, scandione and calophione A. *European Journal of Organic Chemistry* 2014; 2014(12): 2496–2507. doi: 10.1002/ejoc.201301722
16. Richter MJR, Schneider M, Brandstätter M, et al. Total synthesis of (−)-Mitrephorone A. *Journal of the American Chemical Society* 2018; 140(48): 16704–16710. doi: 10.1021/jacs.8b09685
17. Hyatt JL, Stacy V, Wadkins RM, et al. Inhibition of carboxylesterases by benzil (diphenylethane-1,2-dione) and heterocyclic analogues is dependent upon the aromaticity of the ring and the flexibility of the dione moiety. *Journal of Medicinal Chemistry* 2005; 48(17): 5543–5550. doi: 10.1021/jm0504196
18. Ganapaty S, Srilakshmi GVK, Pannakal ST, et al. Cytotoxic benzil and coumestan derivatives from tephrosia calophylla. *Phytochemistry* 2009; 70(1): 95–99. doi: 10.1016/j.phytochem.2008.10.009
19. Babudri F, Fiandanese V, Marchese G, Punzi A. A direct access to α-diones from oxalyl chloride. *Tetrahedron Letters* 1995; 36(40): 7305–7308. doi: 10.1016/0040-4039(95)01471-S
20. Singh SK, Saibaba V, Ravikumar V, et al. Synthesis and biological evaluation of 2,3-diarylpyrazines and quinoxalines as selective COX-2 inhibitors. *Bioorganic & Medicinal Chemistry* 2004; 12(8): 1881–1893. doi: 10.1016/j.bmc.2004.01.033
21. De Luca L, Mezzetti A. Base-free asymmetric transfer hydrogenation of 1,2-di- and monoketones catalyzed by a $(NH)_2P_2$-macrocyclic iron(II) hydride. *Angewandte Chemie* 2017; 56(39): 11949–11953. doi: 10.1002/anie.201706261
22. Dove AP, Li H, Pratt RC, et al. Stereoselective polymerization of *rac*- and *meso*-lactide catalyzed by sterically encumbered *N*-heterocyclic carbenes. *Chemical Communications* 2006; (27): 2881–2883. doi: 10.1039/b601393g
23. Guo L, Gao H, Guan Q, et al. Substituent effects of the backbone in α-diimine palladium catalysts on homo- and copolymerization of ethylene with methyl acrylate. *Organometallics* 2012; 31(17): 6054–6062. doi: 10.1021/om300380b
24. Chen S, Liu Z, Shi E, et al. Ruthenium-catalyzed oxidation of alkenes at room temperature: A practical and concise approach to α-diketones. *Organic Letters* 2011; 13(9): 2274–2277. doi: 10.1021/ol200716d
25. Gao A, Yang F, Li L, Wu Y. Pd/Cu-catalyzed oxidation of alkynes into 1,2-diketones using DMSO as the oxidant. *Tetrahedron* 2012; 68(25): 4950–4954. doi: 10.1016/j.tet.2012.04.069
26. Ren W, Xia Y, Ji SJ, et al. Wacker-type oxidation of alkynes into 1,2-diketones using molecular oxygen. *Organic Letters* 2009; 11(8): 1841–1844. doi: 10.1021/ol900344g
27. Zhao Q, Bai C, Zhang W, et al. Catalytic epoxidation of olefins with graphene oxide supported copper (salen) complex. *Industrial & Engineering Chemistry Research* 2014; 53(11): 4232–4238. doi: 10.1021/ie500017z
28. Shul'pin GB, Mishra GS, Shul'pina LS, et al. Oxidation of hydrocarbons with hydrogen peroxide catalyzed by maltolato vanadium complexes covalently bonded to silica gel. *Catalysis Communications* 2007; 8(10): 1516–1520. doi: 10.1016/j.catcom.2006.12.022
29. Nam W, Kim HJ, Kim SH, et al. Metal complex-catalyzed epoxidation of olefins by dioxygen with co-oxidation of aldehydes. A mechanistic study. *Inorganic Chemistry* 1996; 35(4): 1045–1049. doi: 10.1021/ic950782a
30. Hamilton DE, Drago RS, Zombeck A. Mechanistics Studies on the cobalt (II) Schiff base catalyzed oxidation of olefins by O_2. *Journal of the American Chemical Society* 1987; 109(2): 374–379. doi: 10.1021/ja00236a014
31. Mi C, Meng XG, Liao XH, Peng X. Selective oxidative cleavage of terminal olefins into aldehydes catalyzed by copper (II) complex. *RSC Advances* 2015; 5(85): 69487–69492. doi: 10.1039/c5ra14093e
32. Singla M, Mathur P, Gupta M, Hundal MS. Oxidation of electron deficient olefins using a copper(II) complex based on a bis-benzimidazole diamide ligand. *Transition Metal Chemistry* 2008; 33(2): 175–182. doi: 10.1007/s11243-007-9029-8

33. Wei L, You S, Tuo Y, Cai M. A highly efficient heterogeneous copper-catalyzed oxidative cyclization of benzylamines and 1,3-dicarbonyl compounds to give trisubstituted oxazoles. *Synthesis* 2019; 51(16): 3091–3100. doi: 10.1055/s-0037-1610710
34. Xia J, Huang X, Cai M. Heterogeneous copper(I)-catalyzed cascade addition–oxidative cyclization of nitriles with 2-aminopyridines or amidines: Efficient and practical synthesis of 1,2,4-triazoles. *Synthesis* 2019; 51(09): 2014–2022. doi: 10.1055/s-0037-1611712
35. Dehbanipour Z, Zarnegaryan A. Oxidation of alcohols to carbonyl compounds over graphene oxide functionalized with copper-thiazole as a catalyst. *Inorganic Chemistry Communications* 2023; 155: 110961. doi: 10.1016/j.inoche.2023.110961
36. Lashanizadegan M, Gorgannejad Z, Sarkheil M. Cu (II) Schiff base complex on magnetic support: An efficient nano-catalyst for oxidation of olefins using H_2O_2 as an eco-friendly oxidant. *Inorganic Chemistry Communications* 2021; 125: 108373. doi: 10.1016/j.inoche.2020.108373
37. Kumar R, Mathur P. Oxidation of phenyl propyne catalyzed by copper (II) complexes of a benzimidazolyl Schiff base ligand: Effect of acid/base, oxidant, surfactant and morphology. *Spectrochimica Acta Part A: Molecular and Biomolecular Spectroscopy* 2015; 136: 818–823. doi: 10.1016/j.saa.2014.09.099
38. Zhang G, Yi H, Zhang G, et al. Direct observation of reduction of Cu (II) to Cu (I) by terminal alkynes. *Journal of the American Chemical Society* 2014; 136(3): 924–926. doi: 10.1021/ja410756b
39. Lei J, Sha W, Xie X, Weng WT. Copper-catalyzed C (sp)–H bond hydrazidation. *Organic Letters* 2023; 25(2): 320–324. doi: 10.1021/acs.orglett.2c03876
40. Alvarez LX, Christ ML, Sorokin AB. Selective oxidation of alkenes and alkynes catalyzed by copper complexes. *Applied Catalysis A: General* 2007; 325(2): 303–308. doi: 10.1016/j.apcata.2007.02.045
41. Baiker A, Mallat T. Towards environmentally benign catalytic oxidation. *Catalysis Science & Technology* 2013; 3(2): 267. doi: 10.1039/c2cy90058k
42. Hülsey MJ, Lim CW, Yan N. Promoting heterogeneous catalysis beyond catalyst design. *Chemical Science* 2020; 11(6): 1456–1468. doi: 10.1039/c9sc05947d
43. Kumar R, Mahiya K, Mathur P. Dimeric copper (II) complex of a new Schiff base ligand: Effect of morphology on the catalytic oxidation of aromatic alcohol. *Dalton Transactions* 2013; 42(24): 8553–8557. doi: 10.1039/c3dt50348h
44. Le Bail A, Duroy H, Fourquet JL. Ab-initio structure determination of $LiSbWO_6$ by X-ray powder diffraction. *Materials Research Bulletin* 1988; 23(3): 447–452. doi: 10.1016/0025-5408(88)90019-0.
45. Ma Z, Chu Y, Fu C, et al. The effects of coordinated molecules of two gly-Schiff base copper complexes on their oxygen reduction reaction performance. *Catalysts* 2018; 8(4): 156. doi: 10.3390/catal8040156
46. Kannappan R, Tanase S, Mutikainen I, et al. Square-planar copper (II) halide complexes of tridentate ligands with π–π stacking interactions and alternating short and long Cu⋯ Cu distances. *Inorganica Chimica Acta* 2005; 358(2): 383–388. doi: 10.1016/j.ica.2004.09.003
47. Kumar R, Kumar R, Mahiya K, Mathur P. Oxidation of substituted benzyl amines using a phenoxo-bridged dimeric nickel (II) complex: Synthesis, crystal structure and catalytic activity. *Transition Metal Chemistry* 2015; 40(2): 189–195. doi: 10.1007/s11243-014-9905-y
48. Al-Shamry AA, Khalaf MM, El-Lateef HMA, et al. Development of new azomethine metal chelates derived from isatin: DFT and Pharmaceutical Studies. *Materials* 2022; 16(1): 83. doi: 10.3390/ma16010083
49. Abu-Dief AM, El-Khatib RM, Aljohani FS, et al. Synthesis, structural elucidation, DFT calculation, biological studies and DNA interaction of some aryl hydrazone Cr^{3+}, Fe^{3+}, and Cu^{2+} chelates. *Computational Biology and Chemistry* 2022; 97: 107643. doi: 10.1016/j.compbiolchem.2022.107643
50. Abu-Dief AM, Alotaibi NH, Al-Farraj ES, et al. Fabrication, structural elucidation, theoretical, TD-DFT, vibrational calculation and molecular docking studies of some novel adenine imine chelates for biomedical applications. *Journal of Molecular Liquids* 2022; 365: 119961. doi: 10.1016/j.molliq.2022.119961
51. Abu-Dief AM, El-Sagher HM, Shehata MR. Fabrication, spectroscopic characterization, calf thymus DNA binding investigation, antioxidant and anticancer activities of some antibiotic azomethine Cu(II), Pd(II), Zn(II) and Cr(III) complexes. *Applied Organometallic Chemistry* 2019; 33(8): e4943. doi: 10.1002/aoc.4943
52. Adam MSS, Abdel-Rahman LH, Abu-Dief AM, Hashem NA. Synthesis, catalysis, antimicrobial activity, and DNA interactions of new Cu(II)-Schiff base complexes. *Inorganic and Nano-Metal Chemistry* 2019; 50(3): 136–150. doi: 10.1080/24701556.2019.1672735
53. Ahuja G, Kumar R, Mathur P. Oxidation of olefins catalyzed by Iron (III) complexes of bis-benzimidazolyl diamide ligands. *Journal of Molecular Structure* 2012; 1011: 166–171. doi: 10.1016/j.molstruc.2011.12.047
54. Bakshi R, Kumar R, Mathur P. Oxidation of substituted alkynes catalyzed by a non-heme iron (III) bis benzimidazole diamide complex as catalyst under ambient conditions. *Indian Journal of Chemistry* 2011; 50A(5): 658–663.
55. Kneubühl FK. Line shapes of electron paramagnetic resonance signals produced by powders, glasses, and viscous liquids. *The Journal of Chemical Physics* 1960; 33(4): 1074–1078. doi: 10.1063/1.1731336
56. Roessler MM, Salvadori E. Principles and applications of EPR spectroscopy in the chemical sciences. *Chemical Society Reviews* 2018; 47(8): 2534–2553. doi: 10.1039/c6cs00565a

57. Jeong J, Yoon B, Kwon YW, et al. Singly and doubly occupied higher quantum states in nanocrystals. *Nano Letters* 2017; 17(2): 1187–1193. doi: 10.1021/acs.nanolett.6b04915
58. Kumar R, Yadav A, Mahiya K, Mathur P. Copper(II) complexes with box or flower type morphology: Sustainability versus perishability upon catalytic recycling. *Inorganica Chimica Acta* 2016; 450: 279–284. doi: 10.1016/j.ica.2016.06.012
59. Cheula R, Maestri M, Mpourmpakis G. Modeling morphology and catalytic activity of nanoparticle ensembles under reaction conditions. *ACS Catalysis* 2020; 10(11): 6149–6158. doi: 10.1021/acscatal.0c01005
60. Dong F, Meng Y, Han W, et al. Morphology effects on surface chemical properties and lattice defects of Cu/CeO_2 catalysts applied for low-temperature CO oxidation. *Scientific Reports* 2019; 9(1): 12056. doi: 10.1038/s41598-019-48606-2
61. Li Z, Guo X, Tao F, Zhou R. New insights into the effect of morphology on catalytic properties of MnO_x–CeO_2 mixed oxides for chlorobenzene degradation. *RSC Advances* 2018; 8(45): 25283–25291. doi: 10.1039/c8ra04010a